DISTRIBUTION OF ^{14}C AND ^{13}C IN FOREST SOILS OF THE DINGHUSHAN BIOSPHERE RESERVE

Chengde Shen[1,2,3] • Weixi Yi[1] • Yanmin Sun[1] • Changping Xing[1] • Ying Yang[1] • Chao Yuan[1] • Zhian Li[4] • Shaolin Peng[4] • Zhisheng An[2] • Tungsheng Liu[1]

ABSTRACT. We report here first results on the bulk soil organic carbon (SOC), apparent radiocarbon ages and $\delta^{13}C$ characteristics of the tropical and subtropical forest soil in Dinghushan Biosphere Reserve (DHSBR). The forest oxisol in Dinghushan has developed during the Holocene. The $\delta^{13}C$ variation curves in all three profiles may be divided into two sections. The upper section from 0 to 40 cm has $\delta^{13}C$ values varying from –27.4 to –24.1‰, –27.5 to –22.2‰, and –24.4 to –20.1‰. in the Wukesong, Qingyunsi and Kengkou profiles, respectively. The lower section, including the 40–160 cm horizons, has a uniform $\delta^{13}C$. The mean $\delta^{13}C$ values of the soil organic carbon could be used not only to discriminate between C_3 and C_4 plants, but also to distinguish between coniferous and broad-leaf plants.

INTRODUCTION

Soils receive carbon in the form of vegetation litter and release CO_2 during microbial decay of the litter. The continuous deposition of weathered and fallen plant materials and animal remains, and subsequent decay of this material, makes the pedosphere a very important carbon pool. Therefore, changes in soil organic carbon (SOC) may greatly affect the global concentration of atmospheric CO_2. Both ^{14}C and ^{13}C tracing can help to reveal the dynamics of SOC, including CO_2 exchange between soils and the atmosphere, which may help to identify the "missing sink" of anthropogenic CO_2 released to the atmosphere (Tan et al. 1990; Jenkinson et al. 1991). Here, we present the first results on the bulk SOC, apparent ^{14}C ages, and $\delta^{13}C$ characteristics of the tropical and subtropical forest soil in Dinghushan Biosphere Reserve (DHSBR).

Geological Environment and Soil Profiles

Located in Zhaoqing, Guangdong Province, southern China (23°09′21″–23°11′30″N, 112°30′39″–112°33′41″E), the DHSBR is a forest ecosystem research station of the Chinese Academy of Sciences and the UN-ESCO-MAB Biosphere Reserve Network. The topography of the DHSBR is hilly, dominated by low mountains declining southeastward. Jilong Mountain, with an elevation of 1000 m, is the highest peak, located in the northwest margin of the reserve. The mountains generally have slopes of 30°–40° and Devonian sandy shale dominates the base rock. Forest soil in this area consists mainly of oxisol enriched in humus with a pH of 4.5–5.0. The mean annual temperature of this region is about 21.4 °C, while the mean annual rainfall is about 1927 mm, 69% of which occurs between May and September. The vegetation is tropical monsoon rainy forests and subtropical monsoon evergreen broadleaf forests (Wu et al. 1982; He et al. 1982).

Wukesong, Qingyunsi, and Kengkou soil profiles are selected as the research objects in this work. The Wukesong profile is located at the hillside with an elevation of 315 m and a slope of 28°. The 30–60-cm soil layer is oxisol with organic carbon typically ranging from 1.0 to 0.8%. The vegetation is coniferous and broad-leaf mixed forest. The Qingyunsi profile is situated at a terrace of the foothill with an elevation of 190 m and a slope of 22°. The thick soil layer is oxisol with a middle-high amount of organic matter. The vegetation is monsoon evergreen broadleaf forest. The Kengkou

[1]Guangzhou Institute of Geochemistry, Chinese Academy of Sciences, Guangzhou 510640, China
[2]State Key Laboratory of Xi'an Loess and Quaternary, Chinese Academy of Sciences, Xi'an 710061, China
[3]Corresponding author. Email: cdshen@gig.ac.cn.
[4]South China Institute of Botany, Chinese Academy of Sciences, Guangzhou 510650, China

RADIOCARBON, Vol 43, Nr 2B, 2001, p 671–678
Proceedings of the 17th International ^{14}C Conference, edited by I Carmi and E Boaretto

profile lies in the transition region to DHSBR with an elevation of 42 m and a slope of 28°. The vegetation is *pinus masson* coniferous forest.

The Wukesong soil profile is characterized by visible horizon sequence, thin subsoil, unclear eluvial deposition and has rootlets concentrated within the upper 25 cm of the soil profile. The Qingyunsi profile exhibits thick soil formation with visible horizon sequence, subsoil with clear eluvial deposition (showing organic cutan), forming a block and columnar structure under alternate dry and wet conditions. The Kengkou profile is dominated by a visible horizon sequence, thick subsoil, and rootlets concentrated within the top 10 cm of the soil profile. For these three soil profiles, the granular structure is more obvious in surface horizons, which have medium textures (i.e. loam).

METHODS

After air-drying and picking out visible roots and fragmentary stone, all soil samples were passed through a 1-mm sieve to remove rootlets and coarse sands. All samples were treated with 0.1 N HCl to remove carbonates, and then rinsed with distilled water repeatedly until they became neutral. Soil samples were dried prior to analysis of ^{14}C, ^{13}C, organic carbon, pollen, and opal phytoliths. The samples for ^{14}C measurements were further ground and put into a quartz tube, where they were combusted in an oxygen stream at 800 °C to produce CO_2. The CO_2 was purified repeatedly using dry-ice-acetone and liquid-nitrogen traps and then converted into Li_2C_2 in a Li-reactor under vacuum at 900 °C. Li_2C_2 was hydrolyzed into C_2H_2, which was then synthesized into C_6H_6 under catalysis. ^{14}C measurements were carried out using 1220 Quantulus ultra low level liquid scintillation spectrometer with a scintillation cocktail teflon vial. The natural abundance of ^{13}C is commonly represented by the $\delta^{13}C$ values, calculated according to the equation:

$$\delta^{13}C=[(^{13}C/^{12}C)_{sample} / (^{13}C/^{12}C)_{standard}-1] \times 1000, \quad (1)$$

where $(^{13}C/^{12}C)_{sample}$ is the isotope ratio of the soil organic carbon and $(^{13}C/^{12}C)_{standard}$ is the carbon isotope ratio of the PDB standard. Analysis of soil organic ^{13}C was carried out using a Finnigan Model 251 mass spectrometer with analytical errors lower than 0.2‰. The SOC contents were determined using Heraeus CHN-O elemental analyzer and the routine sulfuric-potassium dichromate method with analytical error lower than 0.04%.

RESULTS AND DISCUSSION

All measurement results for the three soil profiles are listed in Table 1. "Modern" denotes the $\Delta^{14}C$ values higher than zero for the uppermost two soil samples in the Qingyunsi and the Kengkou profiles and the top four soil samples in the Wukesong profile, showing that all of those samples were affected by the "bomb ^{14}C".

Apparent ^{14}C Ages

Only rarely does measurement of soil organic ^{14}C provide a reliable indication of pedogenic chronology. SOC is a complex mixture of compounds entering the soil and being modified during pedogenesis, thus soil organic compounds produced in earlier stage are continuously mixed with those produced in later stage. The measured ^{14}C ages based on the total SOC tend to be younger than pedogenic age, because much of the carbon was only recently deposited in the soil. Hence, the ^{14}C ages of total soil organic carbon are usually referred as apparent ^{14}C ages. SOC can be separated into coarse and fine particle fractions by physical method or decomposed into amino chemical, phenol, polysaccharide and lignin fractions by chemical methods. The oldest ^{14}C ages among soil organic

Table 1 Organic carbon, $\delta^{13}C$ and apparent ^{14}C ages in soil profiles

Lab nr	Field nr	Horizon	Depth (cm)	Organic carbon (%)	$\delta^{13}C$ (‰)	Apparent ^{14}C ages (BP)
Wukesong profile						
GC-96017	I-0	A	0–5	4.19	–27.4	Modern
GC-96016	I-1	A	5–10	2.40	–26.2	Modern
GC-96015	I-2	A/B	10–15	1.79	–24.6	Modern
GC-96014	I-3	A/B	15–20	1.56	–23.9	Modern
GC-96013	I-4	A/B	20–30	1.05	–23.9	442 ± 61
GC-96012	I-5	B	30–40	0.86	–24.1	4858 ± 88
GC-96011	I-6	B	40–50	0.93	–24.1	2281 ± 77
GC-96010	I-7	B	50–60	0.76	–24.6	1605 ± 68
GC-96009	I-8	B/C	60–70	0.63	–24.1	1829 ± 79
GC-96008	I-9	B/C	70–80	0.76	–24.6	2734 ± 83
GC-96007	I-10	B/C	80–100	0.69	–24.4	4102 ± 131
GC-96006	I-11	B/C	100–120	0.61	–24.9	4093 ± 81
GC-96005	I-12	B/C	120–140	0.48	–25.2	4595 ± 81
GC-96004	I-13	B/C	140–160	0.52	–25.0	5572 ± 94
Qingyunsi profile						
GC-96036	II-1	A	0–5	4.73	–27.5	Modern
GC-96037	II-2	A	5–10	3.63	–26.6	Modern
GC-96038	II-3	A	10–15	2.58	–25.5	761 ± 68
GC-96039	II-4	A	15–20	2.06	–24.3	485 ± 66
GC-96040	II-5	A/B	20–25	2.02	–23.1	819 ± 68
GC-96041	II-6	A/B	25–30	1.87	–22.5	762 ± 66
GC-96042	II-7	A/B	30–35	1.78	–23.1	1212 ± 76
GC-96043	II-8	A/B	35–40	1.54	–22.2	1418 ± 75
GC-96044	II-9	B1	40–50	1.26	–23.4	1959 ± 75
GC-96045	II-10	B1	50–60	1.29	–23.7	2064 ± 73
GC-96046	II-11	B2	60–70	1.15	–24.7	2557 ± 73
GC-96049	II-12	B2	70–80	1.39	–24.5	2047 ± 73
GC-96050	II-13	B2	80–100	0.89	–24.7	2595 ± 96
GC-96051	II-14	B/C	100–120	0.91	–25.5	2491 ± 79
GC-96052	II-15	B/C	120–140	0.68	–25.3	5159 ± 83
GC-96053	II-16	B/C	140–160	0.75	–25.3	8663 ± 112
Kengkou profile						
GC-96022	IV-1	A	0–5	2.30	–24.4	Modern
GC-96023	IV-2	A	5–10	1.67	–21.9	Modern
GC-96024	IV-3	A/B	10–20	1.23	–20.3	377 ± 65
GC-96025	IV-4	A/B	20–30	0.84	–20.4	987 ± 71
GC-96026	IV-5	A/B	30–40	0.66	–20.1	1581 ± 71
GC-96027	IV-6	B	40–50	0.55	–20.2	1129 ± 71
GC-96028	IV-7	B	50–70	0.50	–20.3	1431 ± 76
GC-96029	IV-8	B	70–90	0.66	–20.6	1483 ± 72
GC-96030	IV-9	B	90–110	0.52	–21.3	1698 ± 72
GC-96031	IV-10	B/C	110–130	0.65	–22.3	1945 ± 72
GC-96032	IV-11	B/C	130–150	0.67	–21.6	2883 ± 77

fractions are usually regarded as soil ages. Some investigators referred ^{14}C age of total SOC as the mean residence time under steady conditions (Scharpenseel et al. 1992; Wang and Amundson 1996; Trumbore et al. 1989).

As a function of depth, the apparent ^{14}C ages of the SOC in the Wukesong, Qingyunsi, and Kengkou profiles are shown respectively in Figure 1(a), (b), and (c). The variation of apparent ^{14}C ages in the three profiles may approximately be classified into the following three sections. The first section covers the uppermost 10- or 20-cm layer, showing a large amount of organic matter accumulation and a fast decrease in SOC content with depth (see Table 1). The "bomb ^{14}C" could reach this section and the apparent ^{14}C ages of the SOC in this section are modern. The second section dominates the soils between 10- or 20-cm and 40-cm layers, presenting a decreasing organic matter accumulation and a uniform SOC content with depth. The second section is the influence of rootlets and gley water and shows large fluctuations of apparent ^{14}C ages corresponding to the pedogenesis period. The third section is represented by 40–160-cm layers, which exhibit uniform SOC content with depth, indicating that the influences of rootlets and gley water are weak. The apparent ^{14}C ages can be referred as the mean residence times of the SOC. Based on the apparent ^{14}C ages and soil horizons in the profiles, it may be deduced that the duration of forest pedogenesis in Dinghushan region ranged approximately from 500 to 1000 years. As the original isotope compositions in various soil phases is unchanged during pedogenesis (Scharpenseel et al. 1992), the mean residence time of the total SOC could represent the burial ages of the soils or paleosol.

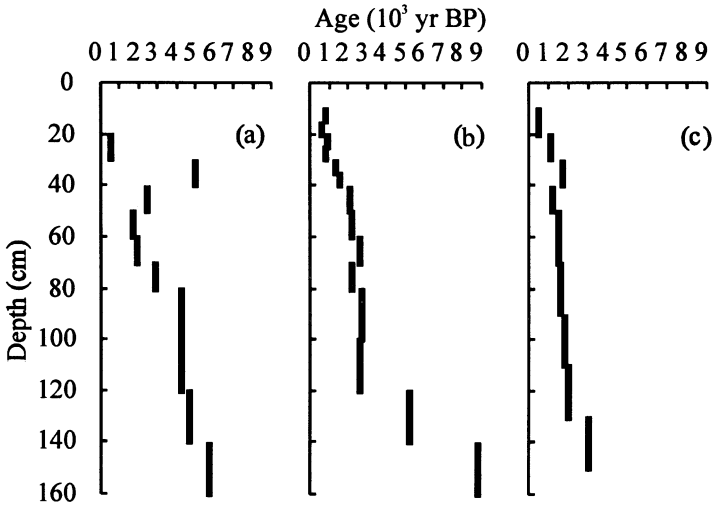

Figure 1 Apparent ^{14}C ages of the soil organic carbon as a function of depth in the Wukesong (a), Qingyusi (b), and Kengkou (c) profiles

$\delta^{13}C$ Distribution Characteristics

Figure 2(a), (b), and (c) show the variations of both $\delta^{13}C$ and SOC contents as functions of depths in the Wukesong, Qingyunsi, and Kengkou profiles, respectively. The depth distribution on both $\delta^{13}C$ and SOC contents show nearly the same patterns although they have different values in the three profiles. For all three profiles, the patterns may be divided into two sections. The first section encompasses the top 35–40 cm of the profiles and corresponds to the pedogenic A and A/B horizons, with $\delta^{13}C$ values varying from −27.4 to −24.1‰, −27.5 to −22.2‰, and −24.4 to −20.1‰ in Wukesong, Qingyunsi and Kengkou profiles, respectively. As soil depth increases, the $\delta^{13}C$ values first increase to reach maximum values, suggesting a progressive $\delta^{13}C$ accumulation, and then grad-

ually decrease to steady values. In this section, the SOC consists of labile constituents with a fast turnover and the content decreases greatly with depth. The second section involves the lowest 120 cm of the profiles (40–60-cm horizons) and corresponds to the pedogenic B and B/C horizons. In this section, the $\delta^{13}C$ values tend to be steady and the SOC consists of refractory constituent. The mean $\delta^{13}C$ values of the SOC in the second sections of the Wukesong, Qingyunsi, and Kengkou profiles are −24.6‰, −24.6‰, and −21.1‰, respectively. This suggests that if there was not a change in the ^{13}C of plant litter inputs, the $\delta^{13}C$ variations of SOC with depths depend mainly on decomposition and turnover of SOC. During pedogenesis, the $\delta^{13}C$ values of the SOC are closely related to soil respiration process such as root and microbe respiration (Cerling et al. 1991; Dorr and Munnich 1980). Of course, since methanogenesis discriminates strongly against ^{13}C, wet soil layers that are an appreciable source of CH_4 might become richer in ^{13}C. The $\delta^{13}C$ variation curves show an enrichment process of ^{13}C during pedogenesis and the degrees of $\delta^{13}C$ enrichment are 3.3‰, 5.3‰, and 4.3‰ in this stage for the Wukesong, Qingyunsi, and Kengkou profiles, respectively.

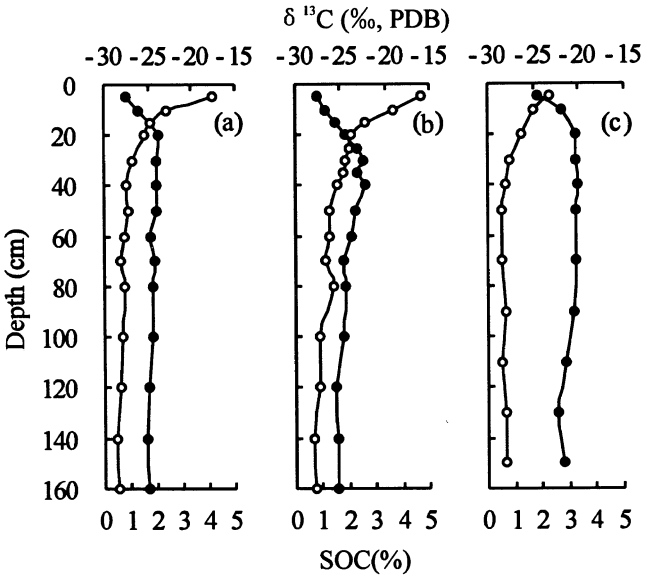

Figure 2 The variations of $\delta^{13}C$ and soil organic carbon contents as a function of depth in the Wukesong (a), Qingyusi (b), and Kengkou (c) profiles. Open circle = organic carbon content; solid circle = $\delta^{13}C$.

$\delta^{13}C$ and Paleo-Vegetation

The atmospheric CO_2 approximately consists of 1.1% ^{13}C and 98.9% ^{12}C. However, the $\delta^{13}C$ value of atmospheric CO_2 has been decreasing from about −6.5‰ before the industrial revolution to −7.8‰ at present because of the burning of fossil fuels and biomass (Becker-Heidmann and Scharpenseel 1989). During the photosynthesis of plants, CO_2 is absorbed by leaves through stoma and is transformed into carboxylic acids under enzyme catalysis. The difference in carbon isotope mass causes isotope fractionation. Thus, the $\delta^{13}C$ of plant tissue may be used to classify natural plants according to photosynthetic pathway, specifically: C_3, C_4, and CAM plants. The $\delta^{13}C$ values range from –34‰ to –23‰ for the C_3 plants, from –22‰ to –6‰ for the C_4 plants, and from –20‰ to –10‰ for the CAM plants (Deines 1980). The C_3 and C_4 or CAM plants could be identified based on their $\delta^{13}C$ values. The $\delta^{13}C$ values of the SOC in the Qingyunsi and Kengkou profiles are compared with those of the prairie soils in Kansas, USA (Cerling et al. 1989) (Figure 3). The vegetation in both Qingyunsi and

Kengkou belong to C_3 plants, while those in the Kansas prairie are C_4 grasses. The difference of mean $\delta^{13}C$ value between them is about 10‰.

There is a difference of about 4‰ between the mean $\delta^{13}C$ values of the Wukesong and Kengkou profiles. Although the vegetation in both profiles are belonged to C_3 plants, the former is coniferous and broadleaf mixed forest and the latter is coniferous forest. The $\delta^{13}C$ values of their litter layers are −27.4‰, −28.7‰, and −24.4‰ for the Wukesong, Qingyunsi, and Kengkou profiles, respectively, which are very close to those of 0–5-cm horizon in each profile. Obviously, the $\delta^{13}C$ values in SOC depend mainly on vegetation species, rather than the $\delta^{13}C$ variations of atmosphere. Although the above discussions refer to the modern vegetation species, $\delta^{13}C$ distribution characteristics in SOC may represent those plants with same $\delta^{13}C$ composition, as evidenced by the pollen analysis results (Bird et al. 1994; Rach and Schlesinges 1992). Balesdent et al. (1993) found that carbon isotope fractionation did not happen during early decomposition of plant litters, and that the turnover time for the SOC in the surface soils were short. Hence, the $\delta^{13}C$ values of the surface soils could be referred to as the representative of the $\delta^{13}C$ values of the surface vegetation. Therefore, if the vegetation has not experienced affection of climate changes and anthropological activities, the $\delta^{13}C$ values of SOC could be used not only to discriminate between C_3 and C_4 plants, but also to identify the coniferous or broadleaf plant species. Because of subtle variations among C_3 forest vegetation, differences in incoming plant ^{13}C at the various sites could have been caused by variations in many factors (Bonal et al. 2000). These include: recycling of soil-derived, plant water stress, sunlight penetration into the canopy, landscape, CH_4 production or consumption by soil and soil parent material. For details on ^{13}C variations among rainforest vegetation still needs to be explored.

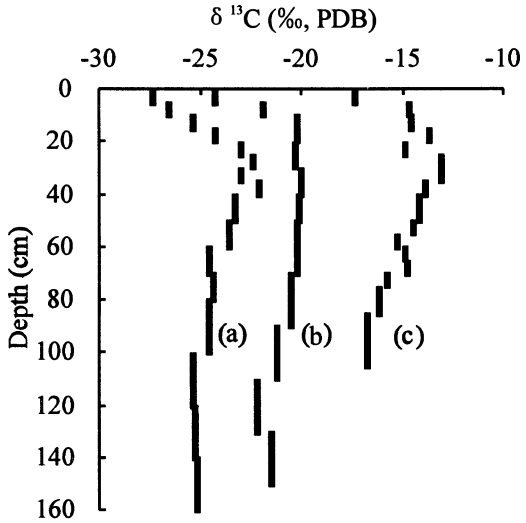

Figure 3 The comparisons of $\delta^{13}C$ variations between forest soil organic carbon from Qingyunsi (a) and Kengkou (b), and prairie soil organic carbon from Kansas, USA (c)

Apparent ^{14}C Ages and Paleo-Environment

The bases of the Wukesong, Qingyunsi, Kengkou soil profiles are very close to the bed-rock, and the maximum of apparent ^{14}C ages of SOC are 5572 ± 94, 8663 ± 112, and 2883 ± 77 yr BP, respectively for these three profiles. As many other factors (e.g. differential leaching of soluble organic C and inheritance of organic C from the Devonian) could influence ^{14}C abundance in the deepest soil layers near bedrock, for short, we refer to interpretation of apparent ^{14}C ages as the time since the forest vegetation was established. If the environment of Dinghushan region has not experienced any

abrupt change during the Holocene, we tend to infer the changes of paleo-environment in this region as follows. The forest oxisol in Dinghushan has developed during the Holocene. The natural forest vegetation occurred in the Qingyunsi area with an elevation of 190 m about 8700 years ago, and then in the Wukesong area with an elevation of 315 m about 5600 years ago. The latter might be associated with the Holocene Megathermal in the East Asia (Shi et al. 1992). Finally, the forest vegetation came up in the Kengkou area with an elevation of 42 m about 2900 years ago. Part of the present coniferous forest in the Kengkou area is obviously related to the anthropogenic activity i.e. reforestation. As seen from the Kengkou soil profile, the mean $\delta^{13}C$ values are –20.5‰ for the upper 10–90-cm horizons and –21.7‰ for the lower 90–150-cm horizons. The more negative $\delta^{13}C$ values of the lower part of the profile might suggest that the vegetation in the Kengkou area was the coniferous and broad-leaf mixed forest in the early period and later became to be the coniferous forest.

CONCLUSIONS

The apparent ^{14}C ages of SOC in three profiles show that forest pedogenesis in the Dinghushan region persisted roughly 500–1000 years. The forest oxisol in the Dinghushan has developed during the Holocene.

The $\delta^{13}C$ variation curves in the three profiles may be divided into two sections. One dominates the uppermost 35–40 cm of the profiles, with the $\delta^{13}C$ values varying between –27.4 and –24.1‰, –27.5 and –22.2‰, and –24.4 and –20.1‰ in the Wukesong, Qingyunsi, and Kengkou profiles, respectively. The other section covers the underlying 120 cm (40–160 cm deep) of the profiles, with the $\delta^{13}C$ values tending to be steady.

The mean $\delta^{13}C$ values of the SOC could be used not only to discriminate between C_3 and C_4 plants, but also to identify signatures of coniferous or broad-leaf plant species.

ACKNOWLEDGMENTS

We thank anonymous referees for extremely thorough and constructive comments on the manuscript. This study was financially supported by NKBRSF Project G1999043401, the Chinese Natural Science Foundation (Grant No. 49973009, 39899370, 49894170, and 49872093), the major and key projects of the Natural Resources and Environment Program, CAS (No. KZ951-A1-402-08-01 and KZ952-J1-402), and the Natural Science Foundation of Guangdong Province (Grant No. 980750 and 980952).

REFERENCES

Balesdent J, Girardin C, Mariotti A. 1993. Site-related $\delta^{13}C$ of tree leaves and soil organic matter in a temperate forest. *Ecology* 74(6):1713–21.

Becker-Heidmann P, Scharpenseel HW. 1989. Carbon isotope dynamics in some tropical soil. *Radiocarbon* 31(3): 672–9.

Bird MI, Haberle SG, Chivas AR. 1994. Effect of altitude on the carbon-isotope composition of forest and grassland soils from Papua New Guinea. *Global Biogeochemical Cycles* 8:13–22.

Bonal D, Sabatier D, Montpied P, Tremeaux D. 2000. Interspecific variability of $\delta^{13}C$ among trees in rainforests of French Guiana: functional groups and canopy integration. *Oecologia* 124:454–68.

Cerling TE, Quade J, Wang Y. 1989. Carbon isotopes in soils and palaeosols as ecology and palaeoecology indicators. *Nature* 341:138–9.

Cerling TE, Solomon DK, Quade J. 1991. On the isotopic composition of carbon in soil carbon dioxide. *Geochemica et Cosmochemica Acta* 55:3403–5.

Deines P. 1980. The isotopic composition of reduced organic carbon. In: Fritz P, Fontes J-Ch, editors. *Handbook of environmental isotope geochemistry. 1: The terrestrial environment*. Amsterdam: Elsevier. p 329–406.

Dorr H, Munnich KO. 1980. Carbon-14 and carbon-13 in soil CO_2. *Radiocarbon* 22(3):909–18.

He CH, Chen SQ, Liang YB. 1982. The soils of Ding Hu Shan Biosphere Reserve. *Tropical and Subtropical Forest Ecosystem* 1: 25–38. In Chinese.

Jenkinson DS, Adams DE, Wild A. 1991. Model estimates of CO_2 emissions from soil in response to global warming. *Nature* 351:304–6.

Raich JW, Schlesinger WH. 1992. The global carbon dioxide flux in soil respiration and its relationship to vegetation and climate. *Tellus* 44(B):81–9.

Scharpenseel HW, Becker-Heidmann P. 1992. Twenty-five years of radiocarbon dating soil: paradigm of erring and learning. *Radiocarbon* 34(3):541–9.

Shi YF, Kong ZC, Wang SM. 1992. The feature of climates and environments of Holocene Megathermal in China. In*:* Shi YF, editor. *The climates and environments of Holocene megathermal in China*. Beijing: China Ocean Press. p 1–18. In Chinese.

Tans PP, Fung IY, Takahashi T. 1990. Observational constraints on the global atmospheric budget. *Science* 247:1431–8.

Trumbore SE, Vogel JS, Southon JR. 1989. AMS ^{14}C measurements of fractionated soil organic matter: an approach to deciphering the soil carbon cycle. *Radiocarbon* 31(3): 644–54.

Wang Y, Amundson R.and Trumbore SE. 1996. Radiocarbon dating of soil organic matter. *Quaternary Research* 45: 282–8.

Wu HS, Deng HZ, Chen HT, Zheng LW. 1982. Physicogeographical features of Ding Hu Shan and their dynamic analyses. *Tropical and Subtropical Forest Ecosystem* 1: 1–10. In Chinese.